Evaluation of the inter- and intrafraction displacement for head patients treated at the particle therapy centre MedAustron based on the comparison of different commercial immobilisation devices

Andrea Zechner[a,*], **Ingrid Ziegler**[b], **Eugen Hug**[a], **Carola Lütgendorf-Caucig**[a], **Markus Stock**[a]

[a] MedAustron Ion Therapy Centre, Wiener Neustadt, Austria
[b] University Clinic for Radiotherapy and Radio-Oncology, Paracelsus Medical University, Salzburg, Austria

Received 29 February 2020; accepted 25 January 2021

Abstract

In December 2016 the clinical operation has started at the particle therapy centre MedAustron, Wiener Neustadt, Austria. Different commercial immobilisation devices are used for head patients. These immobilisation devices are a combination of table tops (Qfix BoS™ Headframe, Elekta HeadStep™), pillows (BoS™ Standard pillow, Moldcare®, HeadStep™ pillow) and thermoplastic masks (Klarity Green™, Qfix Fibreplast™, HeadStep™ iCAST double). For each patient image-guided radiotherapy (IGRT) is performed by acquiring orthogonal X-ray imaging and 2D3D registration and the application of the resulting 6-degree of freedom (DOF) position correction on the robotic couch.

The inter- and intrafraction displacement of 101 adult head patients and 27 paediatric sedated head patients were evaluated and compared among each other regarding reproducibility during the entire treatment and stability during each fraction. For the comparison, statistical methods (Shapiro–Wilk test, Mann–Whitney U-test) were applied on the position corrections as well as on the position verifications. The actual planning target volume margins of 3 mm (adults) and 2 mm (children) were evaluated by applying the van Herk formula on the intrafraction displacement results and performing treatment plan robustness simulations of twelve different translational offset scenarios including a HU uncertainty of 3.5%.

Statistically significant differences between the immobilisation devices were found, but they turned out to be clinically irrelevant. The margin calculation for adult head patients resulted in 0.8 mm (lateral), 1.2 mm (cranio-caudal) and 0.6 mm (anterior–posterior), and for paediatric head patients under anaesthesia in 0.8 mm (lateral), 0.5 mm (cranio-caudal) and 0.9 mm (anterior–posterior). Based on these values, robustness evaluations of selected adult head patients and sedated children showed the validity of the currently used PTV margins.

Keywords: IGRT, Image-guided proton radiotherapy, Interfraction movement, Intrafraction movement, Immobilisation device, Margin, Thermoplastic mask

* Corresponding author: Andrea Zechner, MedAustron Ion Therapy Centre, Wiener Neustadt, Austria.
E-mail: andrea.zechner@medaustron.at (A. Zechner).

Z Med Phys **32** (2022) 39–51
https://doi.org/10.1016/j.zemedi.2021.01.007
www.elsevier.com/locate/zemedi

© 2021 The Author(s). Published by Elsevier GmbH on behalf of DGMP, ÖGMP and SSRMP. This is an open access article under the CC BY-NC-ND license (http://creativecommons.org/licenses/by-nc-nd/4.0/).

1 Introduction

Reproducible patient immobilisation and residual movement management are one of the key topics in radiotherapy regarding positioning and accuracy. In particular, particle therapy is more sensitive to patient movement due to its higher dose gradient at the distal part of the Bragg peak. Therefore, image-guided radiotherapy (IGRT) is an essential component of particle therapy and it is routinely used in clinical practice as well as in high precision photon therapy [1–3].

The reproducibility of the patient setup on a daily basis (interfraction setup accuracy) and the stability of the setup within a fraction (intrafraction setup accuracy) are an indicator of suitable immobilisation equipment. There is literature available for photon therapy [4–7], but only few manuscripts on setup uncertainties in particle therapy [8–10]. The reference [11] provides a detailed summary about patient immobilisation devices as well as recommendations for optimized fixation systems. Several immobilisation systems are commercially available and a few special devices meet the additional requirements for particle therapy. These are, e.g., shallow thickness gradients and table top shapes allowing for minimal airgaps between the patient and the aperture reducing the lateral beam penumbra [12].

An evaluation of patient immobilisation depending on different immobilisation devices was conducted at the particle therapy centre MedAustron (Wiener Neustadt, Austria). The used patient setup verification system is the Imaging Ring (medPhoton GmbH, Salzburg, Austria), which is attached to the ceiling-mounted robotic positioning system [13]. Since the beginning of clinical treatment in December 2016, two different table tops (Qfix BoS^{TM} Headframe, Elekta HeadStep^{TM}), three support cushions (BoS^{TM} Standard pillow, Moldcare$^{®}$, HeadStep^{TM} pillow) and three thermoplastic masks (Klarity Green^{TM}, Qfix Fibreplast^{TM}, HeadStep^{TM} iCAST double) are in use to a different extent. At MedAustron, an isotropic PTV margin of 3 mm and 2 mm, respectively, is applied to the CTV for adult and paediatric head patients. These margins are comparable with currently used margins in proton therapy [14,15].

In photon therapy, the widely used PTV margin formula is based on calculations of systematic and random errors [16]. In proton therapy, a different PTV margin approach, the introduction of a beam-specific margin [17], is proposed for plans with a uniform dose distribution per beam. In case of intensity-modulated proton therapy (IMPT) a scenario-based robustness evaluation is suggested [18]. We combined the PTV approaches from the photon and the proton world and verified our currently applied PTV margins. Therefore, we first determined a margin based on intrafraction displacement results with the van Herk formula [16] and then verified the CTV coverage by calculating different perturbation scenarios including setup and range uncertainties [19].

This paper represents the first report about setup uncertainties of a new facility and compares the immobilisation devices' efficacy among each other. Consequently, based on the inter- and intrafraction displacement results, the exclusion of immobilisation systems with bad performance is considered and furthermore, the actual imaging protocols and frequencies are evaluated at our centre.

2 Materials and methods

The particle therapy centre MedAustron has started clinical operation with protons in December 2016. From the beginning, adult patients with intracranial tumours (e.g. CNS tumors, gliomas, meningeoma), skull base tumours (e.g. chordoma, chondrosarcoma, paraganglioma) and tumours of the paranasal sinus (e.g. SNUC, esthesioneuroblastoma) have been treated using the fixed horizontal proton beam line. In April 2017 the treatment of children (<7 years) under anaesthesia has started and after the vertical beam line commissioning the treatment entities have been extended by pelvic and abdominal adult and paediatric tumour patients.

In this study 101 adult head patients treated with protons between December 2016 and June 2018 and 27 sedated children treated with protons between June 2017 and December 2019 in the head region are included.

All patients went through the same immobilisation procedure and image-guided therapy workflow. The patients received between 1.8 Gray (Gy) and 3 Gy per fraction and the number of fractions ranged between 10 and 30.

2.1 Immobilisation

The commercially available immobilisation devices consist of two different index-capable table tops (Qfix BoS^{TM} Headframe, Elekta HeadStep^{TM}), which are fulfilling the requirements of proton therapy. While the BoS system's shape allows minimizing the distance between the patient and the beam nozzle and therefore decreasing the proton penumbra, the HeadStep provides various positioning possibilities regarding the inclination of the patient's head. Generally, the BoS is chosen in case of superficial targets, for which a range shifter is required, and the air gap reduction becomes an important plan quality criterion. The Headstep table top is considered more stable and is used for cases for which the airgap reduction plays a minor role. The airgap also depends on the couch angle and the achieved airgap ranges between 8 cm and 35 cm.

The choice of the table top automatically determines the pillow (Moldcare$^{®}$, HeadStep^{TM} pillow). The Moldcare is individually formed for each patient and for the HeadStep^{TM} there are different fixed sizes of support cushions available. Three different thermoplastic masks (Klarity Green^{TM}, Qfix Fibreplast^{TM}, HeadStep^{TM} iCAST double) represent the essential immobilisation tool. The possible combinations of table tops, pillows and masks are summarized in Table 1. For

Table 1
Compatibility between table tops, pillows and thermoplastic masks.

Table top	Compatible pillows	Compatible thermoplastic masks
BoS™ Headframe	Moldcare®	Klarity Green™ Qfix Fibreplast™
Elekta HeadStep™	HeadStep™ pillow	HeadStep™ iCAST double

easier readability, from now on, these masks are named Klarity, Kevlar[1] and iCAST, respectively, in this study. The Klarity and the Kevlar masks are compatible with the BoS system and the iCAST mask only attaches to the HeadStep.

Fig. 1 shows the BoS™ Headframe and the Elekta HeadStep™ together with a Moldcare® and a HeadStep™ pillow and a completely mounted system with an iCAST and a Kevlar mask.

The thermoplastic masks Klarity, Kevlar and iCAST were compared with each other regarding their positioning reproducibility and stability. For the investigations of patient movement we distinguished between adult patients and paediatric patients under anaesthesia.

Since there has been no proton gantry in operation at MedAustron, the children were immobilised in different positions (HFS – Head First-Supine, HFP – Head First-Prone, HFDR – Head First-Decubitus Right, HFDL – Head First-Decubitus Left) in order to mimic a gantry and facilitate optimal beam entrance angles, while the adults selected for this study were only immobilised in HFS. That is why several setups were combined for paediatric patients and resulted in more setups than patients (see Table 1). Finally, from the first 1.5 years of clinical operation 101 adult patients were selected for evaluation. The second sample size includes 27 paediatric patients under anaesthesia, who finished their treatment in the period between April 2017 and December 2019. Table 2 is a summary of the patient sample sizes.

2.2 Image-guided therapy workflow

In the treatment room the patient is immobilised on the table attached to the ceiling-mounted 7-DOF robotic positioner [13]. Two orthogonal X-ray images are acquired using the table mounted Imaging Ring [20]. The 2D3D registration software tool automatically registers the planar images to the bony anatomy of the digitally reconstructed radiographs (DRR) of the planning CT. It calculates the 6-DOF (degrees of freedom) position correction, which is transferred to the optically tracked robotic couch moving to the treatment position. The position correction includes three translations (x: lateral (right-left), y: longitudinal (cranio-caudal), z: vertical (anterior–posterior)) and three rotations (pitch, roll, yaw). The clinically allowed commissioned maximum translational and rotational shift is ± 3 cm and $\pm 3^{\circ}$, respectively. During commissioning, the mean deviation in 3D position accuracy of the patient positioner was found to be smaller than 0.5 mm [21,22]. The 2D uncertainty of the imaging system is ± 0.35 mm ($k = 2$) for planar imaging of a treatment volume of ($115 \times 50 \times 40$) cm [13]. Regular quality assurance measurements confirm the Imaging Ring tolerance of max. ± 0.4 mm.

The majority of the treatment plans consists of an alternating set of beams, each with two irradiation fields. The patients always receive initial imaging before the first irradiation field of each fraction. In this study, the time between imaging before the first and the next/last irradiation field is 27 ± 7 min for adult patients and, similarly, 26 ± 7 min in case of children.

The X-ray image acquisition before the fraction is required to correct the patient position. For the first three fractions X-ray imaging is done also after the fraction or, respectively, after the second irradiation field for position verification purposes. After that, depending on the treatment plan and on the physician's decision, either the standard imaging protocol (weekly position verification) or the extended imaging (up to five position verifications per week) protocol is chosen. The intrafraction movement of every patient is analysed on a weekly basis. Fig. 2 presents the entire workflow together with the measures taken in case of inter- and intrafraction movements out of tolerance.

2.3 Patient specific IGRT data

For every patient information about the used immobilisation devices (table top, pillow, mask), the number of fractions, the 6-DOF position correction and verification as the as well as the time between the image acquisition before and after the fraction is collected. The patient specific data allow many analyses: The fraction number together with the position correction before the fraction facilitates conclusions about the interfraction displacement, i.e. variation of the patient position from day to day. The variation of the patient position during the fraction, the intrafraction displacement, is calculated from the difference between the position correction after and before the fraction (position verification). The correlation between intrafraction time, the time interval between the position verifications, and the intrafraction displacement was evaluated via the Pearson's linear correlation coefficient. Based on the inter- and intrafraction displacement numerical results, the immobilisation devices were compared with each other using statistical tests (see Section 2.4). The intrafraction displacement results were used for the calculation of the planning target volume (PTV) margin (see Section 2.5)

[1] The chosen short name for Qfix Fibreplast™ was Kevlar, because the mask consist of the synthetic fiber Kevlar.

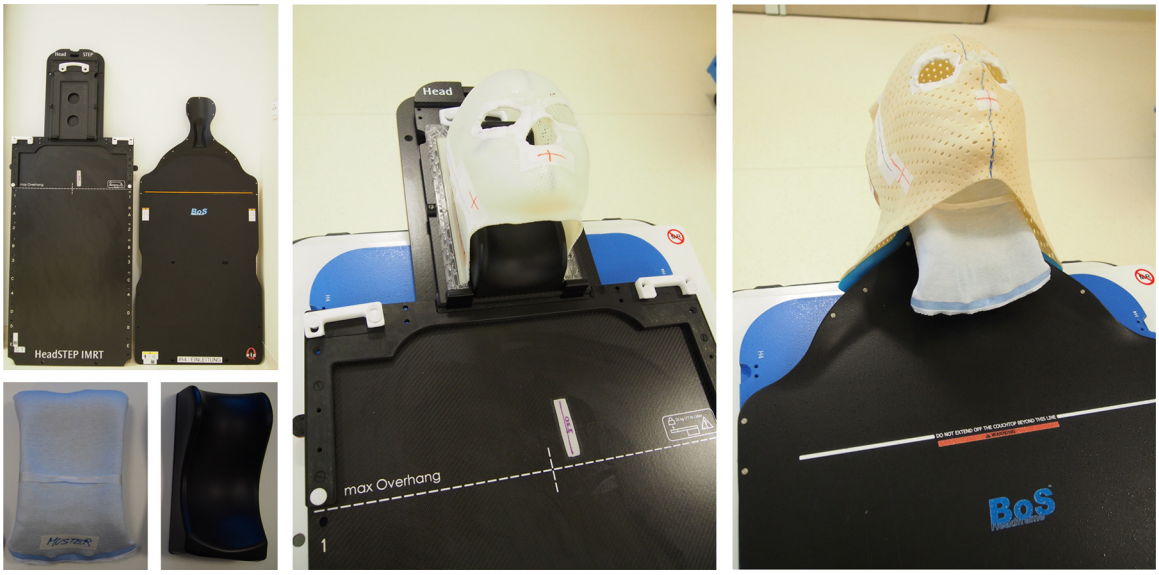

Figure 1. BoS™ Headframe and the Elekta HeadStep™ (top left) together with a Moldcare® and a HeadStep™ pillow (bottom left) and a completely mounted system with an iCAST (middle) and a Kevlar (right) mask.

Table 2
Head patient sample sizes included in the study.

	Timeframe	Patient setup	Masks	Patients	Setups
Adults	December 2016 – June 2018	HFS	Klarity,	101	101
Children	June 2017 – December 2019	HFS, HFP, HFDR, HFDL; sedated	Kevlar, iCAST	27	44

2.4 Statistical tests for immobilisation equipment evaluation

The position correction data enable the statistical comparison of different immobilisation systems. The Shapiro–Wilk test [23–25] was used to determine whether or not the position correction as well as the position verification data follow a normal distribution.

If the normality assumption was not fulfilled, then, in order to compare the group means of the data sets for statistical significance, a one-way ANOVA (analysis of variance) on ranks was performed. This non-parametric method, also called Kruskal–Wallis test, is applicable for more than two groups. It returns the p-value indicating to reject the null hypothesis that all three samples come from the same distribution at a 0.5% significance level. A follow-up test identified the masks, which did not come from the same distribution. These masks were further tested in pairs using the Wilcoxon rank sum test (also known as Mann–Whitney U-test) at 0.5% significance level. Both above mentioned statistical tests allow the comparison of different sample sizes. Moreover, by including the Bonferroni correction for multiple testing the significance level reduced to 0.017%.

If there were no statistically significant differences among the immobilisation types, the intrafraction displacements of the entire sample were used to verify the robustness of the actual margin concept (see Section 2.5).

2.5 Margin evaluation and verification

Following the definitions of van Herk [26], the intrafraction displacements are used to calculate the overall mean (or group systematic) error as well as the systematic and the random errors of the patient cohort. The group systematic error is the mean of all means of the individual patients' intrafraction displacements. The systematic errors, denoted with the capital Sigma Σ, are calculated from the standard deviations (SD) of the means per patient. The random errors, denoted with the lower case σ, are determined by the root mean square of the SDs' of all patients.

The systematic and random errors were inserted into the van Herk formula $2.5\Sigma + 0.7\sigma$ [26] to obtain the PTV margin. The computed margin was used to verify our actual margins (3 mm for adults and 2 mm for paediatric patients). In clinical practice, the treatment plans are generated using a Monte Carlo algorithm (v4.2, Raystation) following the SFO (single field optimization) approach and in special cases the MFO (multi-field optimization) method [27]. Treatment plans of selected head patients with a superficial and, respectively, a deep-seated tumour were evaluated for robustness.

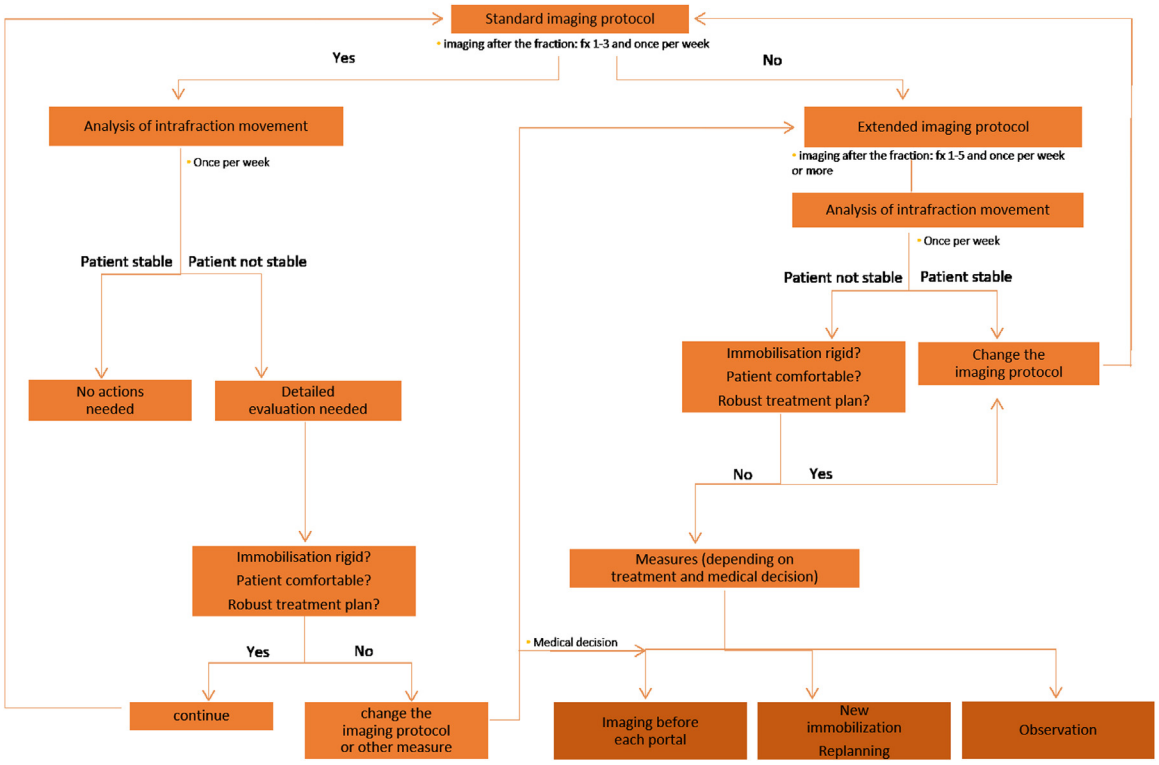

Figure 2. Imaging protocol workflow and decision tree.

Table 3
Interfraction displacement of adult head patients (Klarity (24 setups), Kevlar (56 setups), iCAST (21 setups)) and sedated children (Klarity (3 setups), Kevlar (17 setups), iCAST (24 setups)). The *n* denotes the number of available position correction values.

	Adults			Children (sedated)		
	Median (iqr)					
	Klarity ($n=771$)	Kevlar ($n=1799$)	iCAST ($n=672$)	Klarity ($n=64$)	Kevlar ($n=373$)	iCAST ($n=344$)
Lateral (mm)	0.7 (2.1)	0.8 (2.1)	0.8 (1.7)	−0.2 (5.4)	1.5 (3.9)	0.4 (3.4)
Longitudinal (mm)	−0.9 (4.5)	−0.7 (3.5)	1.0 (2.3)	1.0 (3.3)	0.1 (2.7)	−0.6 (2.4)
Vertical (mm)[a]	n.a.	n.a.	n.a.	n.a.	n.a.	n.a.
Pitch (°)	1.7 (1.3)	1.1 (1.3)	0.5 (1.2)	−0.1 (1.7)	0.3 (1.9)	0.3 (1.2)
Roll (°)	−0.1 (1.3)	0.0 (1.4)	0.1 (1.0)	0.8 (1.8)	−0.2 (1.6)	0.0 (1.3)
Yaw (°)	−0.1 (1.2)	0.0 (1.2)	−0.2 (0.7)	−0.6 (1.6)	−0.4 (1.4)	0.1 (1.7)

n.a.: not applicable.

[a] Due to the table bending and the couch-mounted imaging system the patient's weight and their centre of mass are part of the vertical position correction. The vertical position correction, which is related only to patient setup correction, cannot be differentiated from the weight-dependent correction and evaluated with reasonable certainty and is excluded from the analysis.

Twelve different scenarios were simulated. These scenarios included the calculated margin as shift in positive and negative anterior–posterior, cranio-caudal and left–right direction in combination with a density variation of ±3.5% to account for range uncertainties [26]. The margin was considered as verified, if the clinical target volume (CTV) was covered by 95% of the prescribed dose in all 12 simulated scenarios.

3 Results

3.1 Interfraction displacement

Table 3 shows the position correction values for adult head patients expressed by the median and the interquartile ranges (iqr). For adults, the lateral, roll and yaw components are comparable for all three masks. Klarity and Kevlar perform worse

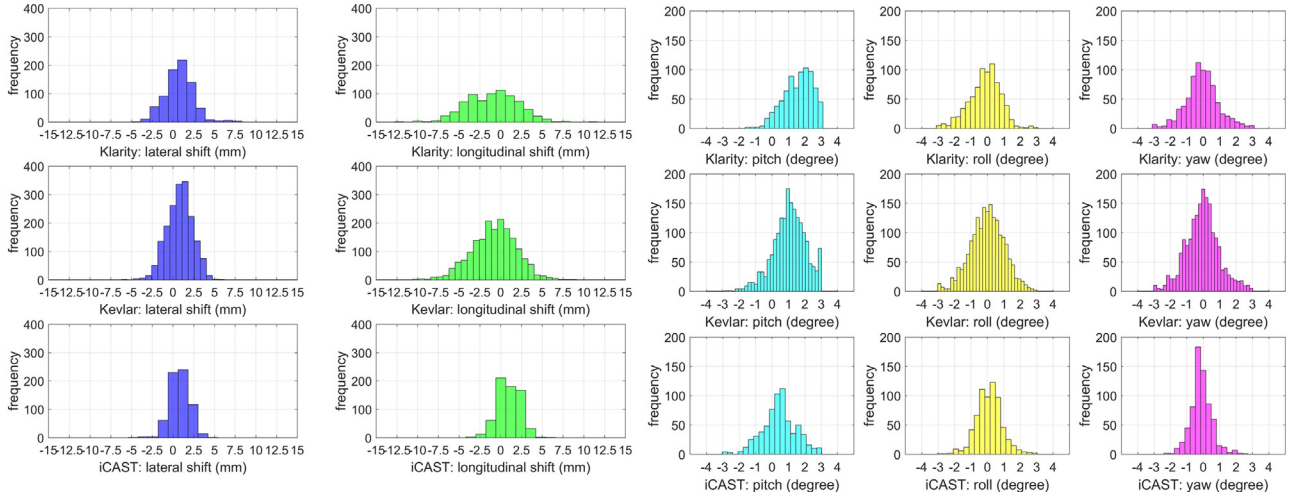

Figure 3. Interfraction displacement: histogram of the position correction for each translation and rotation (adults).

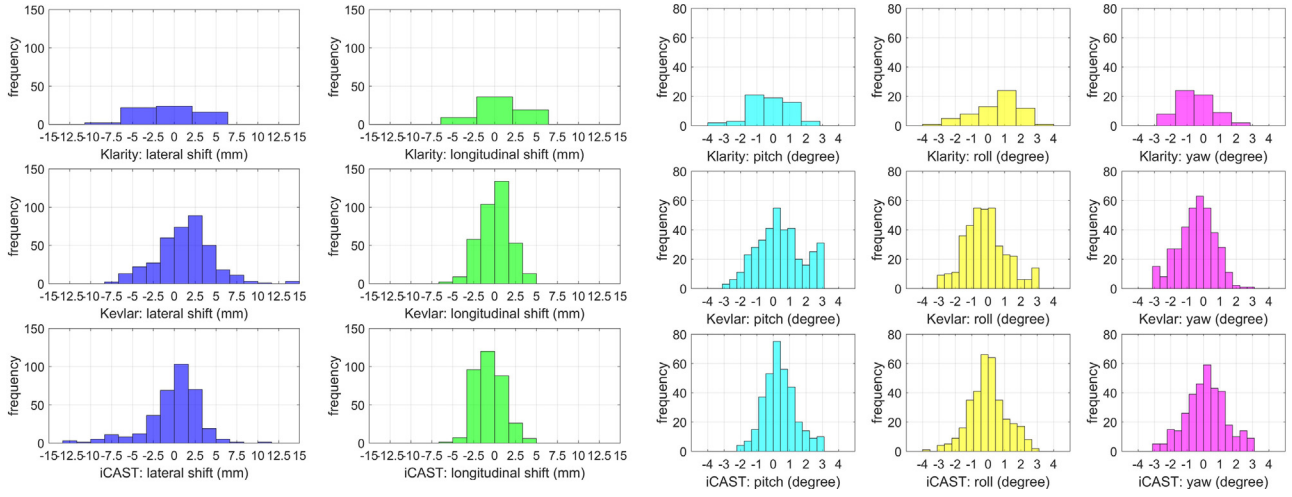

Figure 4. Interfraction displacement: histogram of the position correction for each translation and rotation (children).

than the iCAST in longitudinal direction and pitch rotation. In case of the sedated children, the median and interquartile ranges of all rotational components do not show relevant differences relating to the order of magnitude. For all masks, the median translational values in lateral and longitudinal direction are below a maximum of 1.5 mm, while the interquartile range reaches the maximum of 5.4 mm in case of the Klarity mask.

Figs. 3 and 4 present these data as histograms with the number of bins set equal to the square root of the number of position correction values. The Klarity and the Kevlar mask show a broad distribution over the clinically allowed range in comparison to the narrow plateau-like distribution for the iCAST mask. Their maximum pitch values end at the clinical limit of three degrees and have a distribution, which is skewed to positive values. This indicates high pitch rotations using these masks.

The histograms are summarized for the sedated children as follows (see Fig. 4): The Kevlar and iCAST masks show comparable translational distributions, but in case of the rotations the Kevlar mask reaches higher positive pitch and roll values. The small Klarity mask sample size does not allow a reasonable statement about the distributions.

3.1.1 Statistical analysis of the thermoplastic masks

The non-normality distribution of the interfraction displacement data was determined via the Shapiro–Wilk test and justifies the use of the rank-sum based Wilkoxon test. Table 4 shows the result of pairwise testing of the masks regarding interfraction displacement. All mask pairs that were identified to have a statistically significant difference are listed. They were investigated in detail by evaluating the medians and interquartile ranges (Table 3) and the boxplots (Figs. 5 and 6). In the boxplots, the line in the middle of the box is the median

Table 4
Pairwise testing of statistically significant mask differences regarding interfraction displacement. Mask pairs with statistical differences are shown. As a result from the Wilcoxon test, for these mask pairs the p-value is below 0.017.

Direction	HEAD adults		HEAD children	
	Mask	Mask	Mask	Mask
Lateral	–	–	Klarity	Kevlar
	–	–	Kevlar	iCAST
Longitudinal	Klarity	iCAST	Klarity	iCAST
	Kevlar	iCAST	Kevlar	iCAST
Vertical (n.a.)	–	–	–	–
Pitch	Klarity	Kevlar	Klarity	Kevlar
	Klarity	iCAST	Klarity	iCAST
	Kevlar	iCAST	–	–
Roll	Klarity	Kevlar	Klarity	Kevlar
	Klarity	iCAST	Klarity	iCAST
Yaw	–	–	Klarity	iCAST
	–	–	Kevlar	iCAST

and the diamond symbol is the mean value. The bottom and top of each box are the 25th and 75th percentiles of the sample, respectively. The distance between the bottom and top of each box is the interquartile range. The lines (whiskers) go from the end of the interquartile range to the furthest observation within the whisker length specified as 1.5 times the interquartile range. Observations beyond the whisker length are marked as outliers by the "+" symbol.

The analysis of the position correction values gives information about the constancy and reproducibility of the patients' immobilisation. Therefore, a low interquartile range is favoured over a low median. For both cases, adults and children, the lowest iqr values are present in lateral, longitudinal translation and pitch rotation for the iCAST compared to the Klarity and Kevlar.

3.2 Intrafraction displacement

Table 5 separately shows the medians and interquartile ranges of the position verification results of each mask

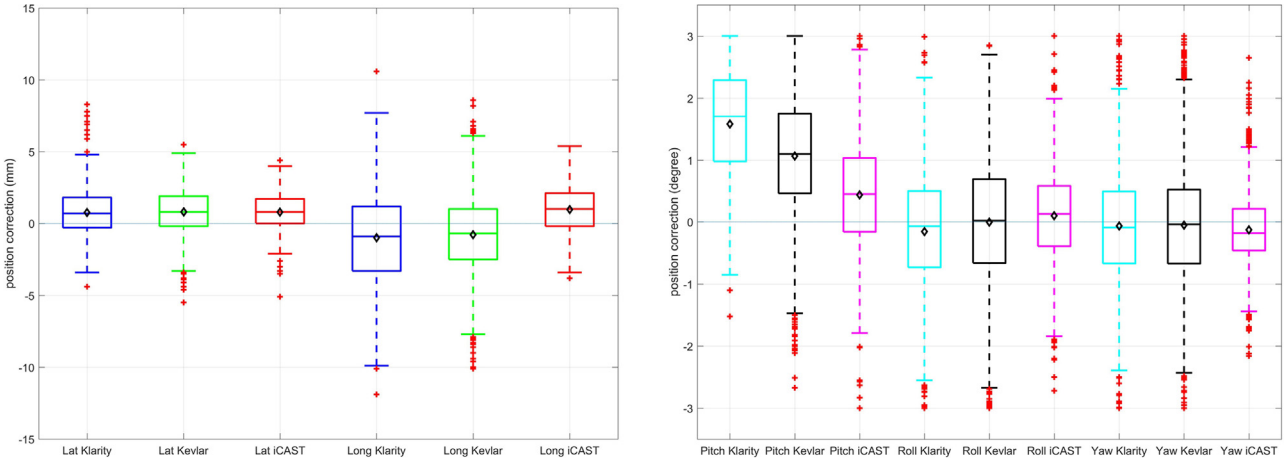

Figure 5. Adult head patients – Boxplot of the interfraction translational and rotational components of the 3 masks.

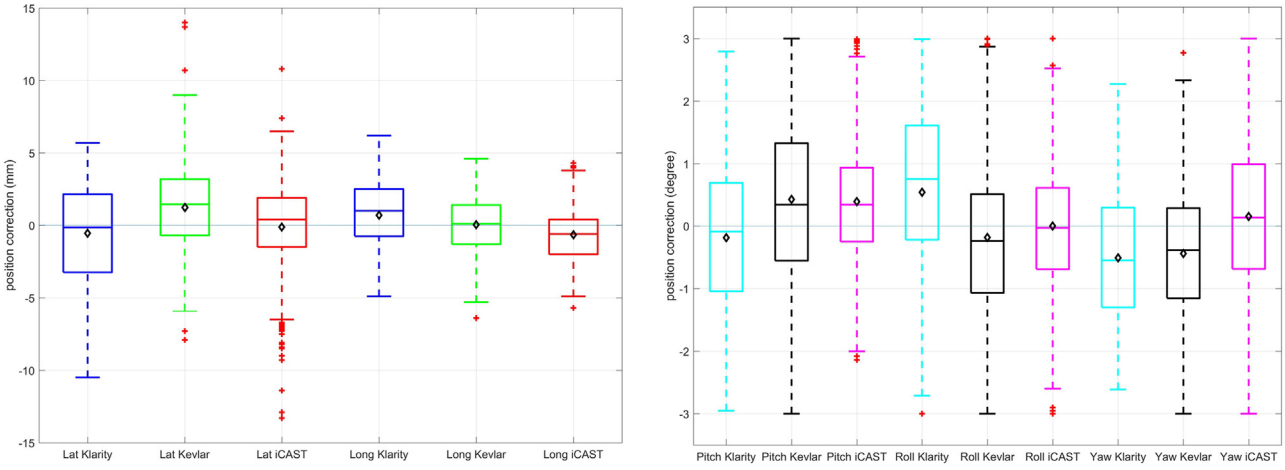

Figure 6. Sedated children – Boxplot of the interfraction translational and rotational components of the 3 masks.

Table 5
Intrafraction displacement results for the three different thermoplastic masks (Klarity (24 setups), Kevlar (56 setups), iCAST (21 setups)) and sedated children (Klarity (3 setups), Kevlar (17 setups), iCAST (24 setups)). The *n* denotes the number of available position verification values.

	Adult			Children		
	Median (iqr)					
	Klarity ($n=229$)	Kevlar ($n=565$)	iCAST ($n=172$)	Klarity ($n=15$)	Kevlar ($n=99$)	iCAST ($n=92$)
Lateral (mm)	0.0 (0.5)	0.0 (0.5)	0.0 (0.3)	0.0 (0.3)	0.0 (0.2)	0.0 (0.2)
Longitudinal (mm)	0.3 (0.8)	0.1 (0.8)	0.0 (0.4)	0.2 (0.3)	0.2 (0.4)	0.0 (0.3)
Vertical (mm)	−0.2 (0.5)	−0.2 (0.4)	0.1 (0.3)	0.0 (0.4)	−0.1 (0.2)	−0.1 (0.2)
Pitch (°)	0.2 (0.9)	0.0 (0.6)	0.0 (0.3)	0.0 (0.3)	0.0 (0.2)	0.0 (0.2)
Roll (°)	0.0 (0.4)	0.0 (0.3)	0.0 (0.3)	0.1 (0.4)	0.0 (0.2)	0.0 (0.2)
Yaw (°)	0.0 (0.5)	0.0 (0.5)	0.0 (0.3)	−0.1 (0.3)	0.0 (0.2)	0.0 (0.2)

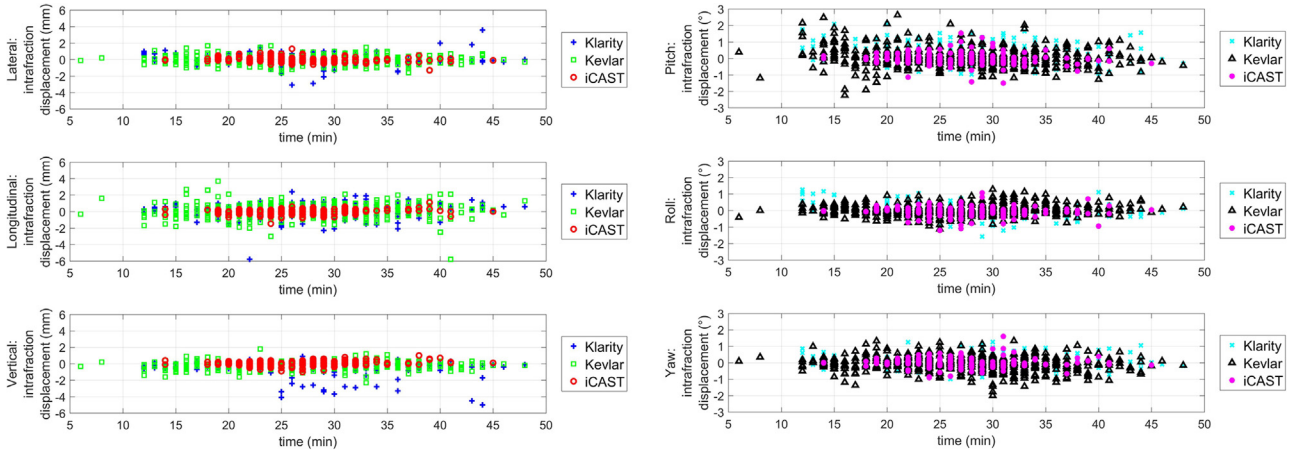

Figure 7. Intrafraction displacement for each translation and rotation dependent on the treatment time and mask (adults).

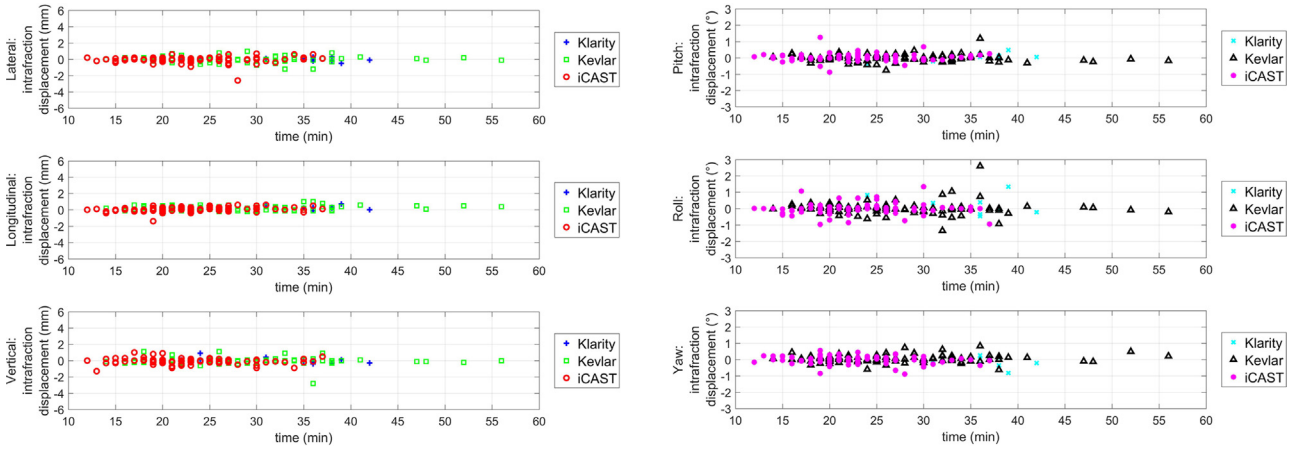

Figure 8. Intrafraction displacement for each translation and rotation dependent on the treatment time and mask (children).

system with different sample sizes. For adults, Klarity and Kevlar show the highest median (iqr) for longitudinal direction and Klarity for the vertical direction. In case of the children, the mask systems do not differ considerably from each other.

Figs. 7 and 8 plot the influence of the intrafraction time (time interval between the position verifications) on the intrafraction displacement. The Pearson's linear correlation coefficient between the time interval between the positon verifications and the intrafraction displacement resulted in approximately

Table 6
Pairwise testing of statistically significant differences between the mask systems regarding intrafraction displacement. Mask pairs with statistical differences are shown. As a result from the Wilcoxon test, for these mask pairs the p-value is below 0.017.

Direction	Adults		Children	
	Mask	Mask	Mask	Mask
Lateral	Klarity	Kevlar	–	–
Longitudinal	Klarity	iCAST	Klarity	iCAST
	Kevlar	iCAST	Kevlar	iCAST
Vertical	Klarity	iCAST	–	–
	Kevlar	iCAST	–	–
Pitch	Klarity	Kevlar	–	–
	Klarity	iCAST	–	–
Roll	Klarity	iCAST	–	–
	Kevlar	iCAST	–	–
Yaw	Klarity	Kevlar	Klarity	Kevlar

zero for the three translations and the three rotations. Hence, neither for adults nor for children, a correlation between intrafraction movement and the treatment time is identifiable.

3.2.1 Statistical analysis of the thermoplastic masks

The Shapiro–Wilk test confirmed that the intrafraction displacement values did not follow a normal distribution. As a consequence, the chosen statistical test to compare the intrafraction displacement of the different masks was based on rank sums (Wilkoxon). Table 6 shows the results of the pairwise testing of statistically significant differences between the masks. All mask pairs were identified to have a statistically significant difference. They were cross-checked with the imaging system accuracy regarding clinical relevance by evaluating the medians and interquartile ranges (Table 5) and the boxplots (Figs. 9 and 10).

The analysis of the intrafraction displacement gives information about the stability of the patient's immobilisation within a fraction. Therefore, a low median and interquartile range are preferred. For adults, this is true for the longitudinal and the vertical component of the iCAST in contrast to the Klarity and Kevlar. In case of the children, all mask systems have a median (iqr) less or equal ±0.2 mm (<0.4 mm) (translations) and ±0.1° (<0.4°) (rotations).

Fig. 11 shows histograms of the 3D vector length of the three different masks for adults (left) and children (right). In all cases the 95% confidence interval is higher than the imaging ring system measurement uncertainty (see Section 2.2).

3.3 Margin calculation

Based on the intrafraction displacement data of all 101 adult head setups ($n = 966$) and 44 children head setups ($n = 206$), the overall mean, the group systematic and the random error and consequently, the margin are calculated. Table 7 presents the results for the three translational directions.

3.4 Robustness

Fig. 12 shows the dose volume histograms (DVH) of two adult head patients with a superficial and, respectively, a tumour in the centre. The dashed line is the unperturbed nominal case, for which no setup shifts and HU uncertainties are applied. The solid lines represent the twelve perturbation scenarios with the calculated setup margin (see Table 7) and 3.5% HU uncertainty. The grey vertical dotted line is the 95% isodose value of the prescribed dose. In all simulated perturbed scenarios, the CTV dose coverage is within 95%.

4 Discussion and conclusion

The evaluation of interfraction displacements of adult and paediatric sedated head patients favours the HeadStep™ iCAST double mask over the Klarity Green™ and Qfix Fibreplast™ mask, which show a broader distribution of position correction values as well as larger pitch values. In general,

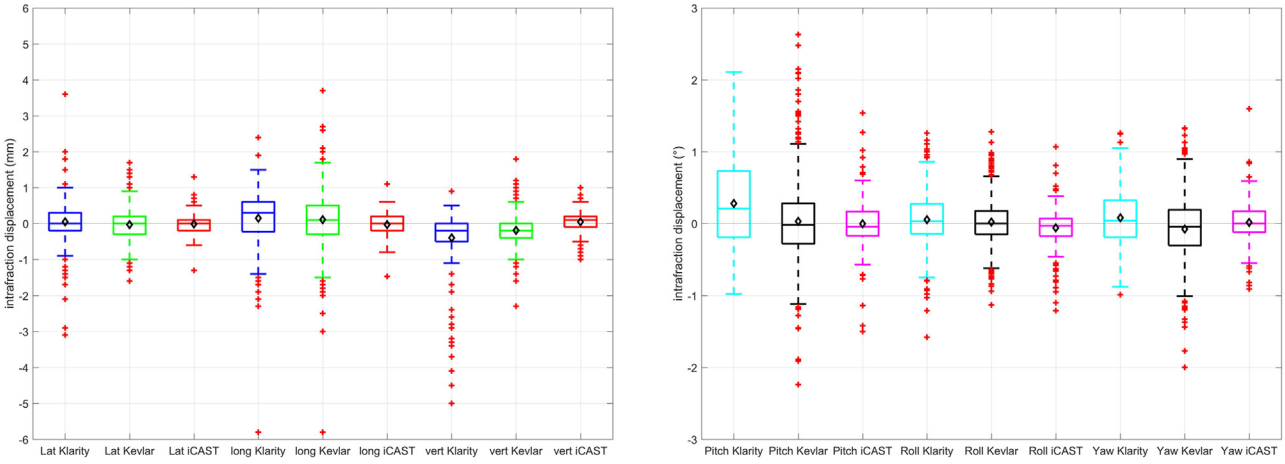

Figure 9. Boxplot of the intrafraction displacement of adult head patients immobilised with the different masks.

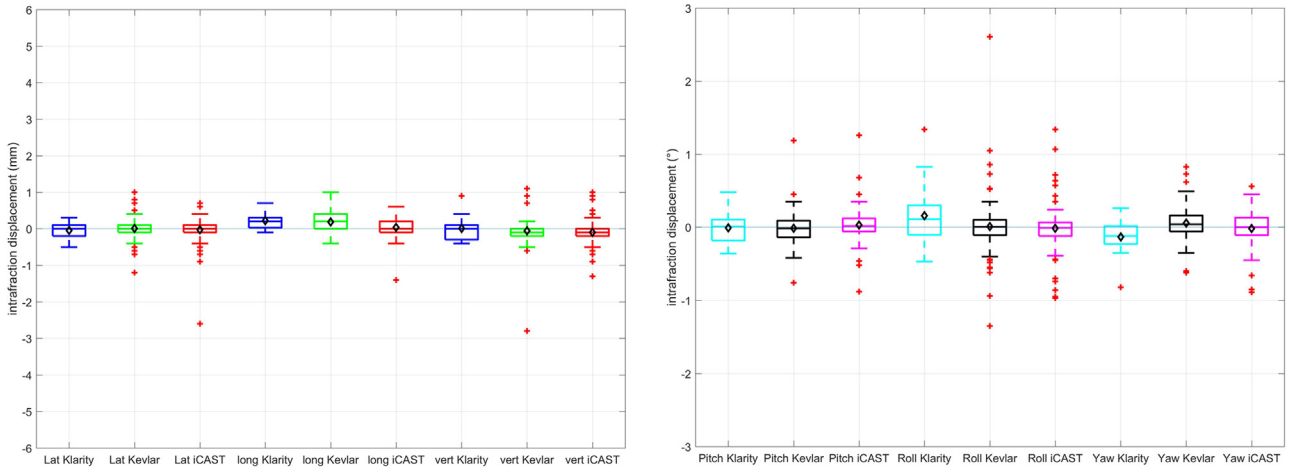

Figure 10. Boxplot of the intrafraction displacement of paediatric sedated patients immobilised with the different masks.

Table 7
Overall mean, systematic and random errors and margin for adults and children.

		Mean M (mm)	Systematic error Σ (mm)	Random error σ (mm)	Margin (mm)
Adults	Lateral	0.0	0.3	0.4	0.9
($n = 966$)	Longitudinal	0.1	0.4	0.6	1.4
	Vertical	−0.2	0.3	0.3	1.0
Children	Lateral	0.0	0.2	0.3	0.6
($n = 206$)	Longitudinal	0.1	0.2	0.2	0.6
	Vertical	−0.1	0.2	0.4	0.8

the HeadStep^{TM} iCAST mask performs best regarding low median and interquartile range for adult patients. The median and interquartile range do not differ among the masks for children. Although the children are immobilised under anaesthesia, the reproducibility of the position is not better than for the adults. Actually, it is slightly better in case of the pitch rotation, but it is worse in case of the lateral component, which shows approximately the doubled interquartile range. One reason for the reproducibility weakness might be the missing feedback from the sedated patients if the setup feels comfortable and is consistent with previous treatments. Another reason might be the different sedated patient positions (HFS, HFP, HFDR, HFDL), which are not necessarily equally reproducible.

In case of adult patients and their intrafraction displacements the masks are numerically comparable regarding rotations, while the Klarity Green^{TM} and Qfix Fibreplast^{TM} have the highest intrafraction displacement for the longitudinal direction with a median (iqr) of 0.3 mm (0.8 mm) and 0.1 mm (0.8 mm), respectively. The median (iqr) intrafraction displacement of the children agree within maximum 0.2 mm (0.4 mm) (translations) and 0.1° (0.4°) (rotations) for all 6 degrees-of-freedom. Hence, no clear distinction between the masks can be made.

On the one hand, the intrafraction displacement data contain information about the patient movement, even though the timestamp of a possible movement remains unknown, and on the other hand a residual error from the registration and imaging device accuracy. No time dependency on the intrafraction displacement could be observed despite longer times, 27 min on average, between the position verifications.

The thermoplastic masks were compared with each other regarding their position correction and their position verification values. Statistically significant differences were found between the masks. For interfraction displacement the most noticeable differences exist between the Klarity/Kevlar and the iCAST mask for the longitudinal translation and the pitch rotation.

Regarding intrafraction displacement, for adults, the HeadStep^{TM} iCAST double also provides better results for longitudinal translation and pitch rotation, while the statistically significant differences between Klarity Green^{TM} and Qfix Fibreplast^{TM} are clinically irrelevant.

Since there is only a limited combination of immobilisation devices possible, e.g. Elektra Head Step^{TM} – Head Step^{TM} pillow – Head Step^{TM} cast double mask or Fix Boss^{TM} Headframe – Medicare® – Clarity Green^{TM}/Fix Fibroblast^{TM}, differences among the masks might also be due to the pillow type. Furthermore, the selection of the table top is dependent on the treated tumour site and its location within the head. As a first step, the Klarity Green^{TM} mask was taken out of the clinically used mask pool, because of the slightly

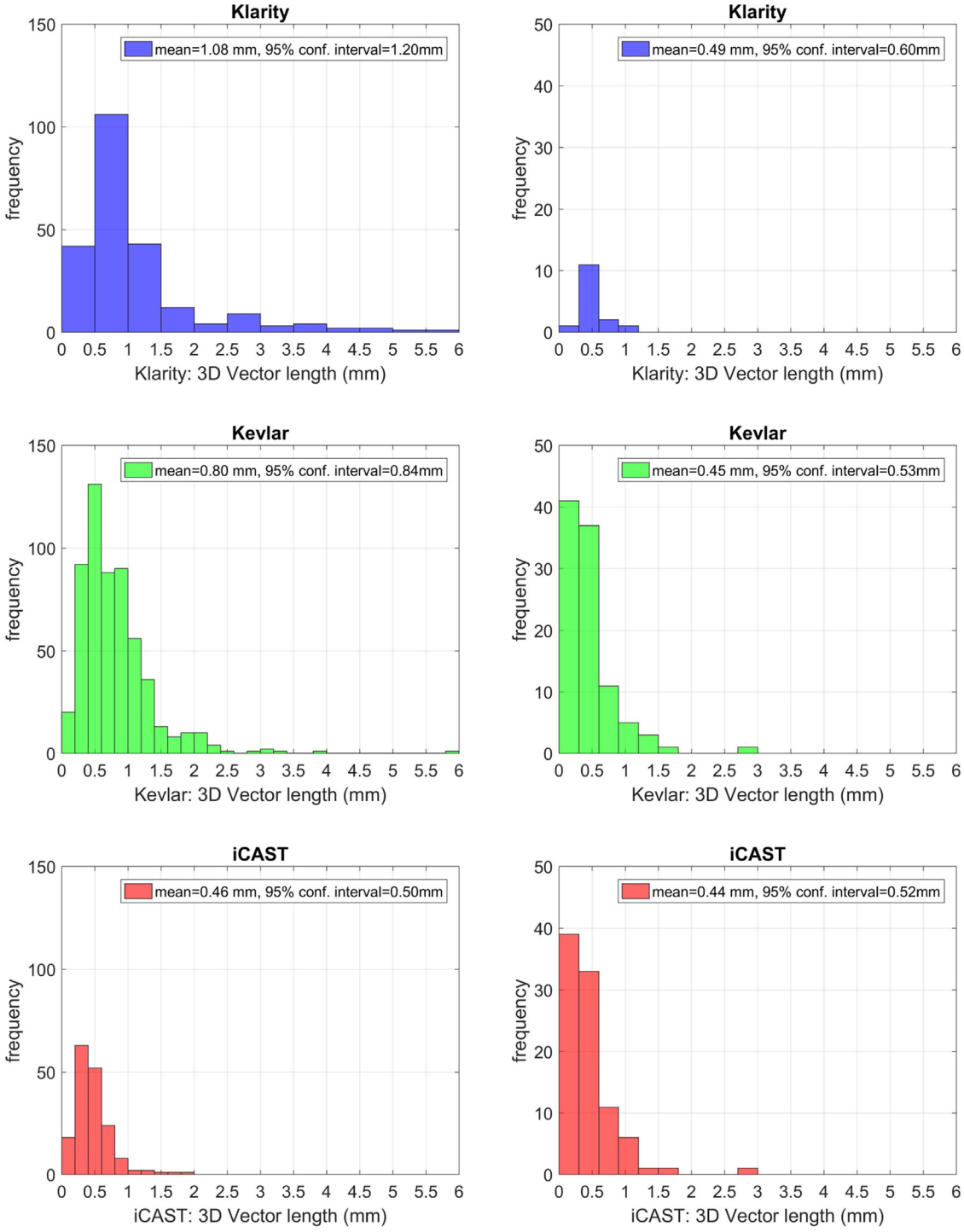

Figure 11. 3D vector length for the three different masks for the entities adult head (left) and children (right).

worse results and its material was subjectively felt to be too soft.

Our intrafraction displacement and margin results are comparable with studies from Amelio 2013 [8] (adult head patients) and Beltran 2011 [9] (paediatric patients under anaesthesia). The computed setup margins in Ref. [8] are 1.0 mm (lateral), 1.3 mm (longitudinal) and 1.0 mm (vertical) in comparison with our results 0.9 mm (lateral), 1.4 mm (longitudinal) and 1.0 mm (vertical). In Ref. [9] the setup and residual uncertainty for children treated with

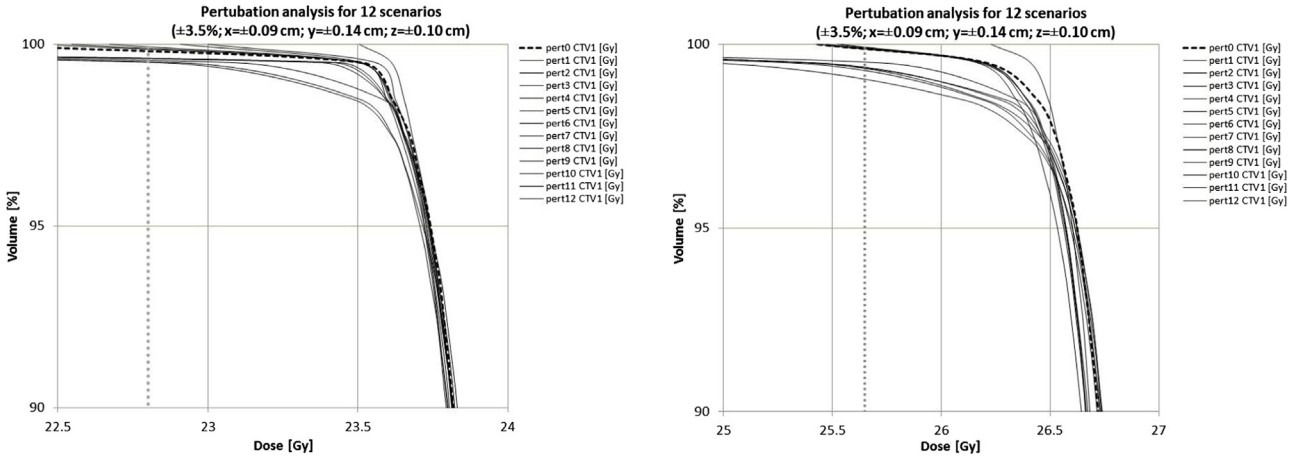

Figure 12. DVHs of the simulated 12 perturbation scenarios for head patients with a superficial tumour (left) and the tumour in the head centre (right). The "pert0" (dashed line) represents the nominal plan; the other lines represent 12 perturbations for the CTV. The curves "pert1" to "pert12" include combinations of single translational shifts and HU uncertainties in positive and negative direction.

anaesthesia is 1.3 mm (lat), 1.5 mm (long) 1.6 mm (vert), which is slightly higher than our margin calculation (0.6 mm, 0.6 mm, 0.8 mm). However, when using daily position correction based on CBCT, they also conclude a PTV margin of 2 mm for children in supine position.

All the recorded data are not only used for retrospective evaluations, but also for online surveillance of the patient's position stability and offline evaluations. On a weekly basis the position verification data of all patients under treatment are analysed based on a script and represented graphically. Patients, for which inter- and intrafraction displacement is out of machine and internal intrafraction movement tolerances (1/3 and 2/3 of the PTV margin), or show a systematic or random behaviour, are discussed in weekly meetings between the physicians, medical physicists and radiation therapy technologists. The actions depend on the possible reasons for patient movement, which can be related to the patient compliance, the immobilisation, the image registration or the imaging protocol. Possible actions are then to comfort the patient, to slightly adapt the immobilisation devices, to review the imaging parameters (viewing angles, X-ray tube settings) or to change the imaging frequency (see workflow chart Fig. 2). A further measure is to evaluate the treatment plan robustness by recomputing the plan including the intrafraction displacement and perform evaluations of additional dose to the OARs and the over- or underdosage of the CTV. Clinically relevant influences of intrafraction patient displacement triggers position correction before each irradiation field, re-immobilisation or robust re-planning. Generally, per week, these measures are applied for 15% of the patients under treatment.

An additional secondary result of this study is the evaluation of the imaging frequency for adults and children under anaesthesia. It should be kind of obvious to have no intrafraction displacement for sedated patients and indeed, the results confirm this assumption. On the other hand, it is rather surprising to detect also single intrafraction displacement of paediatric patients larger than 1 mm and/or 1°. This indicates a kind of (passive) movement during the sedation. Consequently, the imaging frequencies following the standard or the extended imaging protocol remain unchanged for the time being for adults as well as for children.

For the sake of completeness, three remaining uncertainties are pointed out: Residual uncertainties affecting the registration accuracy due to human factors (inter- and intraobserver variation) are estimated to be about ±0.2 mm. Secondly, each of the 6-DOF position correction element is separately analysed, although these values are not independent from each other. Finally, it should be noted that the comfort factor for the patient factor was not explicitly surveyed, but no significant positive or negative feedback was provided.

The margin, which is necessary to cover uncertainties based on intrafraction displacements, was calculated using the van Herk formula. For selected patient cases, a robust evaluation was done by calculating the CTV coverage for twelve different perturbation scenarios including ±3.5% HU range uncertainties. Considerations of the machine tolerances of the MedAustron therapy accelerator were based on key commissioning results as well as beam stability trend lines after more than two years of operation [28]. Daily quality assurance measurements of the beam range and beam position show a mean deviation of 0.5 mm from the baseline data. This beam uncertainty cannot be resolved in our treatment planning system (CT resolution 0.7 mm × 0.7 mm × 1.0 mm) and the contribution of patient setup uncertainties dominates over the machine tolerances. The estimation of the machine uncertainty was considered as sufficient within the frame of this work, and will be monitored for more detailed accuracy investigations. It was concluded that the CTV was covered by 95% of the dose prescription and therefore the actual applied PTV margins of 3 mm (adults) and 2 mm (children)

are appropriate regarding the CTV coverage and treatment accuracy.

Conflict of interests

The authors declare that they have no known competing financial interests or personal relationships that could have appeared to influence the work reported in this paper.

References

[1] Zelefsky MJ, Kollmeier M, Cox B, Fidaleo A, Sperling D, Pei X, et al. Improved clinical outcomes with high-dose image guided radiotherapy compared with non-IGRT for the treatment of clinically localized prostate cancer. Int J Radiat Oncol Biol Phys 2012;84:125–9.

[2] Wang D, Zhang Q, Eisenberg BL, Kane JM, Li XA, Lucas D, et al. Significant reduction of late toxicities in patients with extremity sarcoma treated with image-guided radiation therapy to a reduced target volume: results of radiation therapy oncology group RTOG-0630 trial. J Clin Oncol 2015;33:2231–8.

[3] Engels B, Soete G, Gevaert T, Storme G, Michielsen D, De Ridder M. Impact of planning target volume margins and rectal distention on biochemical failure in image-guided radiotherapy of prostate cancer. Radiothe Oncol 2014;111:106–9.

[4] Rosewall T, Chung P, Bayley A, Lockwood G, Alasti H, Bristow R, et al. A randomized comparison of interfraction and intrafraction prostate motion with and without abdominal compression. Radiother Oncol 2008;88:88–94.

[5] Tryggestad E, Christian M, Ford E, Kut C, Le Y, Sanguineti G, et al. Inter- and intrafraction patient positioning uncertainties for intracranial radiotherapy: a study of four frameless, thermoplastic mask-based immobilization strategies using daily cone-beam CT. Int J Radiat Oncol Biol Phys 2011;80(1):281–90.

[6] Poulsen PR, Muren LP, Høyer M. Residual set-up errors and margins in on-line image-guided prostate localization in radiotherapy. Radiother Oncol 2007;85:201–6.

[7] Schmidhalter D, Malthaner M, Born EJ, Pica A, Schmuecking M, Aebersold DM, et al. Assessment of patient setup errors in IGRT in combination with a six degrees of freedom couch. Z Med Phys 2014;24:112–22.

[8] Amelio D, Winter M, Habermehl D, Jäkel O, Debus J, Combs SE. Analysis of inter- and intrafraction accuracy of a commercial thermoplastic mask system used for image-guided particle radiation therapy. J Radiat Res 2013;54:i69–76.

[9] Beltran C, Krasin M, Merchant T. Inter- and intrafractional positional uncertainties in pediatric radiotherapy patients with brain and head and neck tumors. Int J Radiat Oncol Biol Phys 2011;79(4):1266–74.

[10] Ricotti R, Pella A, Tagaste B, Elisei G, Fontana G, Bonora M, et al. Long-time clinical experience in patient setup for several particle therapy clinical indications: management of patient positioning and evaluation of setup reproducibility and stability. Br J Radiol 2020;93:1107.

[11] ULICE (Union of Light-Ion Centres in Europe): D.JRA 5.1 – Recommendations for optimized fixation systems, WP 5 – Adaptive treatment planning for ion radiotherapy.

[12] Engelsman M, Mazal A, Jaffray D-A. Patient positioning and set-up verification for planning and treatment. In: Proton and charged particle therapy. 1st edition; 2008.

[13] Stock M, Georg D, Ableitinger A, Zechner A, Utz A, Mumot M, et al. The technological basis for adaptive ion beam therapy at MedAustron: status and outlook. Z Med Phys 2018;28(August (3)):196–210.

[14] Albertini F, Hug E, Lomax A. Is it necessary to plan with safety margins for actively scanned proton therapy? Phys Med Biol 2011;56:4399–413.

[15] Beltran C, Roca M, Merchant TE. On the benefits and risks of proton therapy in pediatric craniopharyngioma. Int J Radiat Oncol Biol Phys 2012;82(2):e281–7.

[16] Van Herk M, Remeijer P, Rasch C, Lebesque J. The probability of correct target dosage: dose-population histograms for deriving treatment margins in radiotherapy. Int J Radiat Oncol Biol Phys 2000;47(4):1121–35.

[17] Park P, Zhu X, Lee A, Sahoo N, Melancon A, Zhang L, et al. A beam-specific planning target volume (PTV) design for proton therapy to account for setup and range uncertainties. Int J Radiat Oncol Biol Phys 2012;82(February (2)):e329–36.

[18] Korevaar E, Habraken S, Scandurra D, Kierkels RGJ, Unipan M, Eenink MGC, et al. Practical robustness evaluation in radiotherapy – a photon and proton-proof alternative to PTV-based plan evaluation. Radiother Oncol 2019;141:267–74, http://dx.doi.org/10.1016/j.radonc.2019.08.005.

[19] Paganetti H. Range uncertainties in proton therapy and the role of Monte Carlo simulations. Phys Med Biol 2012;57:R99–117.

[20] Zechner A, Stock M, Kellner D, Ziegler I, Keuschnigg P, Huber P, et al. Development and first use of a novel cylindrical ball bearing phantom for 9-DOF geometric calibrations of flat panel imaging devices used in image-guided ion beam therapy. Phys Med Biol 2016;61(22):N592–605.

[21] Ableitinger A, Utz A, Zechner A, Vatnitsky S, Stock M. Commissioning of a robotic patient positioning system equipped with an integrated tracking system. Radiother Oncol 2017;123(Suppl. 1). S958.

[22] Utz A, Ableitinger A, Zechner A, Mumot M, Teichmeister M, Steininger P, et al. Quality assurance of a novel table mounted imaging device integrated in a patient positioning system. Radiother Oncol 2017;123(Suppl. 1):S261.

[23] Royston P. An extension of Shapiro and Wilk's W test for normality to large samples. J Roy Stat Soc Ser C 1982;31(2):115–24.

[24] Royston P. Approximating the Shapiro–Wilk *W*-test for non-normality. Stat Comput 1992;2:117–9.

[25] Royston P. A toolkit for testing non-normality in complete and censored samples. J Roy Stat Soc Ser D 1993;42(1):37–43.

[26] Van Herk M. Errors and margins in radiotherapy. Semin Radiat Oncol 2004;14(January (1)):52–64.

[27] Quan EM, Liu W, Wu R, Li Y, Frank SJ, Zhang X, et al. Preliminary evaluation of multifield and single-field optimization for the treatment planning of spot-scanning proton therapy of head and neck cancer. Med Phys 2013;40(August (8)):081709.

[28] Grevillot L, Osorio Moreno J, Letellier V, Dreindl R, Elia A, Fuchs H, et al. Clinical implementation and commissioning of the MedAustron Particle Therapy Accelerator for non-isocentric scanned proton beam treatments. Med Phys 2020;47(February (2)):380–92.

Available online at www.sciencedirect.com

ScienceDirect